

## Article

# Ultrasound-Assisted Cold Alkaline Extraction: Increasing Hemicellulose Extraction and Energy Production from Populus Wood

S. Lozano-Calvo , J. M. Loiza , J. C. García , M. T. García and F. López

Research Centre for Technology of Products and Chemical Processes (PRO2TECS), Department of Chemical Engineering, University of Huelva, Av. 3 de marzo s/n, 21071 Huelva, Spain; javiermauricio.loiza@diq.uhu.es (J.M.L.); juan.garcia@diq.uhu.es (J.C.G.); mtrinidad.garcia@diq.uhu.es (M.T.G.); baldovin@diq.uhu.es (F.L.)

\* Correspondence: susana.lozano@diq.uhu.es

**Abstract:** Alkaline pretreatments are considered highly effective for the separation of the different components of lignocellulosic biomass. However, cold alkaline extraction (CAE) exhibits minimal modification/degradation of hemicellulosic fraction and successfully accomplishes efficient delignification. In this research, the fast-growing clone AF2 of *Populus x euramericana* wood was utilized as the raw material and subjected to ultrasound-assisted CAE. The objective of incorporating ultrasound into cold alkaline extraction is to increase the yield of a hemicellulosic-rich liquid phase that can be used to produce high-value products such as furfural or xylitol. Simultaneously, it aims to obtain a solid phase with a higher calorific value compared to the raw material. The results, obtained from a central composite factorial design, demonstrated that the CAE process for 90 min at a sodium hydroxide concentration of 100 g L<sup>-1</sup>, a temperature of 30 °C, and with ultrasound assistance maximized hemicellulose extraction in the liquid phase (60.8% was extracted) and improved the heating value of solid phase.

**Keywords:** biomass; delignification; hemicelluloses; pre-treatment; ultrasound



**Citation:** Lozano-Calvo, S.; Loiza, J.M.; García, J.C.; García, M.T.; López, F. Ultrasound-Assisted Cold Alkaline Extraction: Increasing Hemicellulose Extraction and Energy Production from Populus Wood. *Forests* **2024**, *15*, 109. <https://doi.org/10.3390/f15010109>

Academic Editor: Sabrina Palanti

Received: 11 December 2023

Revised: 24 December 2023

Accepted: 30 December 2023

Published: 5 January 2024



**Copyright:** © 2024 by the authors. Licensee MDPI, Basel, Switzerland. This article is an open access article distributed under the terms and conditions of the Creative Commons Attribution (CC BY) license (<https://creativecommons.org/licenses/by/4.0/>).

## 1. Introduction

International commitments of the European Union to mitigate climate change have promoted a search for clean, renewable energy sources including biomass [1]. More than 60% of the amount of energy produced from biomass in the world is obtained from renewable sources, which account for up to 19.3% of the whole energy output [2]. The use of lignocellulosic biomass has expanded steadily in recent times and is expected to continue to grow in the coming years by virtue of the value-added products that can be obtained from chips, pellets, biogas, and other biorefinery materials [3,4]. However, conventional agroforestry systems cannot by themselves meet the growing demand, so fast-growing woody species are being increasingly planted for this purpose [5]. In this scenario, converting biomass through biorefinery processes has a high potential judging by their sustainability, and also by the fact that they use waste materials to provide alternative energies and high value-added products according to the principles of sustainable development [6,7]. In addition, commitments to a circular economy, the need to reduce the dependence on raw materials from non-renewable fossil resources, and the consequences of climate change all necessitate the adoption of novel technologies within conventional production sectors. This transition aims to supplant the prevailing industrialization model with efficient use of natural resources as far as possible [8,9].

A number of plant species of the genera *Populus*, *Salix*, *Eucalyptus*, *Miscanthus*, *Cynara*, *Paulownia*, *Robinia*, *Casuarina*, and *Leucaena*, among others, are being used as short-rotation energy crops on a global scale [6,10,11]. Some are multi-purpose species that provide a

variety of goods such as forage or paper pulp, and services such as soil restoration or carbon sequestration. These industrial lignocellulosic crops are expected to cover 5–10% of the global forest area by 2050 [12]. In Europe alone, farmland has undergone degradation to such an extent that 45% of its soils have low organic matter contents (<2%); also, 15% have problems due to over-fertilization with inorganic nitrogen, and more than 147 million hectares are seriously eroded [13]. Fortunately, at least 70% of all degraded land is under a climate allowing plants such as *Robinia pseudoacacia*, *Ulmus pumila*, *Eucalyptus* sp., and/or *Populus* sp. to grow. It can thus be useful to assess biomass production, industrial use, and the environmental impact of their intensive production on already poor, degraded soils with a view to their potential exploitation [14]. The limited research carried out in this area has indicated that the results are influenced by specific plant species, cultivation conditions, and environmental factors [15,16].

Recent studies have shown the genus *Populus* can easily adapt to varying environmental conditions; also, it possesses a high hybridization capacity and ease of vegetative propagation. These advantages, together with its fast growth, have boosted the development of a very broad clonal offer that allows clones to be selected for optimal growth at specific sites and for specific purposes [11].

The principal components of lignocellulosic biomass are cellulose, hemicellulose, and lignin. All of these components have the potential to yield high-value products. However, achieving this goal necessitates the utilization of a biorefinery scheme for the selective separation and recovery of these fractions [17]. Often, it is particularly useful to carry out the fractionation in two steps. The first step involves hydrolysis under relatively mild conditions to extract the hemicelluloses (which have low resistance). Additionally, this helps prevent excessive degradation of cellulose fibers. The second step involves oxidative delignification or organosolv treatment to remove the lignin fraction [18]. Among the various pretreatment methods available, alkaline pretreatment offers significant advantages, including the use of environmentally friendly and non-corrosive chemicals, as well as milder operating conditions [19]. Cold Alkaline Extraction (CAE) is one such pretreatment that offers the added benefit of yielding hemicelluloses for use as food additives or in the production of furfural and polymers [12]. The CAE, conducted at 20–40 °C, does not necessitate high pressures, resulting in reduced energy consumption [20]. Nevertheless, the primary advantage of CAE compared to other biomass fractionation techniques lies in its capacity to selectively extract hemicelluloses with minimal degradation and enable straightforward separation through alcoholic precipitation [21].

However, CAE has its disadvantages, and the most significant one is likely its efficiency, which strongly depends on the specific raw material. This pretreatment has been extensively studied for various applications, and it has been observed that the extraction of hemicelluloses is more efficient in herbaceous lignocellulosic materials than in wood [21–24].

The pretreatment's effectiveness can be enhanced through supplementary procedures, including prehydrolysis, impregnation, or novel techniques such as ultrasound-assisted extraction, sub-critical and supercritical fluid extraction, microwave-assisted extraction, or solvent-accelerated extraction [25,26]. The application of ultrasound can be employed as either a pretreatment step or during the treatment process, providing a clean and eco-friendly extraction method with several benefits [25,27]. Extraction is improved by the transmission of ultrasound, which induces acoustic cavitation. This, in turn, triggers the spontaneous creation of microbubbles. When these microbubbles collapse, they produce localized shock waves and hot spots, releasing high temperatures and pressure. This disintegrates the crystalline structure of solid particles [28]. Ultrasound-assisted fractionation improves the efficiency of conventional processes, and results in a high product yield and selectivity [29]. A. García et al., 2011 [29] investigated various lignocellulosic biomass fractionation processes with ultrasound assistance. The results showed that this technology produced a liquid richer in hemicelluloses and lignin compared to when it was not used.

On the other hand, direct combustion is a method for generating chemical energy. This process leads to the emission of CO<sub>2</sub>, particulate matter, sulfur dioxide, and other compounds. However, the quantities released are relatively lower than those produced by the combustion of fossil fuels [30,31].

There are numerous scientific investigations on the extraction of hemicellulosic derivatives using various alkaline processes, both with and without ultrasound assistance [32,33]. In this work, we combined a cold alkaline treatment with ultrasound technology. This approach lacks references in the literature, representing a significant aspect of academic originality and scientific novelty. Furthermore, the efficiency of CAE is highly dependent on the raw material used, adding another point of scientific and academic novelty when testing these processes on a raw material such as the AF2 clone of *Populus x euramericana*. To the best of the authors' knowledge, there are no bibliographic references exploring its utilization for the simultaneous valorization of the hemicellulosic liquid and energy application of the solid residue, despite numerous studies on the value-added product of hemicellulosic, as demonstrated by A. Tareen et al., 2020 [34]. The AF2 clone of *Populus x euramericana* is a high-yield energy crop, and optimizing the conditions for the industrial biorefinery process holds great potential, especially for potential scaling to a semi-industrial or industrial level of exploitation.

For these purposes, the AF2 clone of *Populus x euramericana* was evaluated as a raw material for hemicellulose extraction using CAE, both with and without ultrasound assistance. The process included modeling and optimization through multiple regression, a widely employed approach for optimizing biomass and waste stream valorization [35,36]. The aim was to obtain a high-value liquid fraction and energy from the resulting solid residue, within the context of comprehensive utilization (biorefining).

## 2. Materials and Methods

### 2.1. Characterization and Storage of Raw Materials

The raw material utilized was wood from the AF2 clone of *Populus x euramericana*, from the province of Huelva, located in southwestern Spain. The material was subject to cold grinding in a Resch mill for 4 min and then sieved to obtain chips approximately 1–3 cm long and 0.5 cm wide. These chips were allowed to equilibrate with ambient moisture and temperature before being stored in tightly closed containers during the period between obtaining the wood chips and their use in the CAE process.

For characterization, the chips were further ground to a size of less than 0.5 mm using an Ika Werke mill. Tests were conducted following international standards, including TAPPI T264 cm-07 for moisture [37], TAPPI 211 om-02 for ash [38], and TAPPI T204 cm-07 in combination with Soxhlet extraction (95% ethanol, 5 h) for extractives [39].

Following gravimetric testing, the material was subjected to quantitative acid hydrolysis with 72% H<sub>2</sub>SO<sub>4</sub>, and the hydrolysate was analyzed for monomeric sugars (glucose, xylose, and arabinose) according to TAPPI T249 cm-09 [40]. This analysis was conducted using high-performance liquid chromatography (HPLC) with an AMinex HPX-87H ion-exchange column (Bio-Rad Laboratories, Alcobendas, Madrid, Spain) at 30 °C as the stationary phase and 0.005 M H<sub>2</sub>SO<sub>4</sub> at a flow rate of 0.6 mL min<sup>-1</sup> as the mobile phase [41]. Klason lignin was determined following the guidelines of TAPPI T222 om-11 [42].

### 2.2. Cold Alkaline Extraction (CAE) with and without Ultrasound

Hemicelluloses were subjected to CAE in a Power Sonic Series 500 ultrasonic bath, using a constant liquid/solid ratio of 15 Kg of water per kg of raw material on a dry basis (odb). The independent operational variables of the process were temperature (20, 30, or 40 °C), time (30, 60, or 90 min), and sodium hydroxide concentration (80, 100, or 120 g L<sup>-1</sup>).

The resulting CAE liquor was filtered, and the solid residue was washed with water. Then, the solid fraction was air-dried to determine moisture content and weighed to calculate the process yield. The solid fraction underwent chemical characterization using the same test as the raw material. Additionally, it was analyzed for calorific value following

CEN/TS 14918:2005 E [43] and UNE 16001 EX [44]. This analysis used a Parr 6300 automatic Isoperibol calorimeter (Parr Instrument Company, Moline, IL, USA), a CGA 540 connector, 99.5% pure oxygen, and a maximum pressure of 2500 psig. Furthermore, the solid was subjected to elemental analysis (C, N, O, and H) using a C/H/S-Analyser autosampler Eltra Helos.

The statistical dispersion of the results from chemical and energetic characterization will not be analyzed using the typical parameters of univariate statistics (standard deviation). As this is a multivariate modeling approach aimed at replicating experimental results, it is important to take into account the dispersion between the experimental values and those calculated using the models detailed in Section 2.3, expressed in terms of the coefficient of variation. The analysis and discussion of this coefficient will be conducted in the results section.

### 2.3. Modeling and Optimization by Multiple Regression-Experimental Design

The CAE process was modeled by multiple regression with provision for linear, quadratic, and interaction terms among the independent variables:

$$Y = a_0 + \sum_{i=1}^n b_i X_{ni} + \sum_{i=1}^n c_i X_{ni}^2 + \sum_{i=1, j=1}^n d_{ij} X_{ni} X_{nj} \quad (i < j) \quad (1)$$

The number of tests needed was decreased and covariance between variables was reduced by using a central composition design with  $N$  tests such that  $N = 2^n + 2 \cdot n + n_c$ ,  $2^n$  being the number of points constituting the design,  $2 \cdot n$  that of axial points and  $n_c$  that of central points. The effect of the different ranges spanned by the variables was suppressed by normalizing their values to 0, 1, and  $-1$  with the following equation:

$$X_n = \frac{X - \bar{X}}{(X_{\max} - X_{\min})/2} \quad (2)$$

where  $X$ ,  $\bar{X}$ ,  $X_{\max}$ , and  $X_{\min}$  represent the value of a particular independent variable, and its mean, maximum, and minimum values, respectively. The dependent variables under examination included yield, glucan, xylan, Klason lignin, and lower heating value (LHV).

The statistical models developed in this study to represent the various dependent variables should exhibit globally significant model values, such as the R-squared ( $R^2$ ) and Snedecor F statistics, that are sufficiently high for the models to have statistical relevance. The “appropriate” threshold for these statistics will vary depending on the type of results and models used, whether working with variables of a more “social” nature or more deterministic ones, as in laboratory experiments. However, in the context of our study, values of  $R^2$  greater than 0.85 and Snedecor F values above 5 are considered very appropriate. In the results section, the statistical significance of each model will be addressed according to these criteria. Furthermore, the statistical importance of each coefficient associated with the independent variables will be evaluated. In this context, a conventional criterion is used, which considers an independent variable to be statistically significant in the model when its significance level “p” is less than 0.05 or the value of the Student- $t$  test is greater than 2. The variables included in the models presented in the results section adhere to this conventional criterion.

Furthermore, in order to simplify interpretation, polynomial equations were employed to generate response surfaces. These surfaces were created by plotting two of the three independent process variables on two horizontal axes while displaying the maximum and minimum levels of the third independent variable. This enables a comprehensive representation of the entire range of variation for each dependent variable in relation to all independent process variables (in our case, alkali concentration, treatment time, and temperature).

### 3. Results and Discussion

The initial hypothesis was that the cold alkaline extraction (CAE) of clone AF2 of *Populus x euramericana* would be more efficient than that of other woody species such as eucalyptus (the reference species here). Furthermore, it was hypothesized that the use of ultrasound during the process would result in increased extraction of hemicelluloses in the liquor. If the process were highly selective for hemicelluloses, there would be the additional benefit of an increased calorific value in the solid residue from CAE. This hypothesis was tested by analyzing the raw material and modeling the results obtained with and without ultrasound for comparison.

#### 3.1. Chemical Characterization of the Raw Material

As previously mentioned, *Populus x euramericana* is a tree species with a wide range of clones [45,46]. In this work, we selected clone AF2 due to its fast growth and adaptability. Under the conditions described above, this clone yielded over 25 tons of dry biomass per hectare per year when harvested at 3-year intervals. The biomass used in this study primarily consisted of stems and branches with a thickness of 2.5–10.0 cm, accounting for 67.5% of the total biomass. The bark content of the biomass, which should ideally be minimized to maintain quality, ranged from 31% in the thickest stems to 12% in those 5.0–10.0 cm thick. The primary criterion for selecting this poplar clone was its sustainability as a crop. Indeed, after 9 years, the target plantation had significantly improved soil quality by increasing the organic matter content by 0.23 percentage points (from 0.80% -typical values in poor soils- to 1.03%) and the nitrogen content by 0.03 percentage points (from 0.12% to 0.15%).

Table 1 displays the results of chip characterization and compares them with the results from Constantí et al., 1998 [47] for the *Populus* genus and those from studies on other lignocellulosic raw materials conducted elsewhere. These results represent various raw materials obtained prior to the extraction process and were acquired by different authors following international standards (TAPPI standards). The table also shows the higher heating value (HHV) for the clone and the other materials. Additional determinations for AF2 included the contents of extractives soluble in 1% NaOH (22.3%, -1.95-), hot water (4.22%, -0.12-), and ethanol–acetone mixtures (2.8%, -0.15-). The similarity between the content of xylan and that in NaOH-soluble extractives suggests that the hemicellulose fraction of the studied clone is primarily composed of that polysaccharide. The elemental composition of the biomass was 6.11% hydrogen (H), 0.00019% sulfur (S), 48.67% carbon (C), and 44.13% oxygen (O).

As shown in Table 1, the lignin and xylan contents of the clone exceeded those of most of the species compared, especially the reference material (*E. globulus*) and the *Populus* species examined by Constantí et al., 1998, and Ebringerová et al., 2010 [47,48]. These differences are quite normal as the materials had different natures despite their common origin. In line with the results of Constantí et al., 1998, and Ebringerová et al., 2010 [47,48], clone AF2 contained no arabinan. Additionally, its  $\alpha$ -cellulose and glucan contents were slightly lower, yet still similar to those of *E. globulus* and those reported by Constantí et al., 1998, and Ebringerová et al., 2010 [47,48] for a different *Populus* species. In contrast, the higher heating value (HHV) significantly exceeded that of most of the other materials, including *E. globulus*.

#### 3.2. Cold Alkaline Extraction of Hemicelluloses with and without Ultrasound Assistance

Table 2 presents the yields, glucan, xylan, and lignin results obtained at each point in the experimental design for the CAE process with and without ultrasound. The values in the table are expressed as a percentage of each polymer in the initial raw material. They could be converted into percentages relative to the raw material by multiplying the value by the corresponding amount in the initial raw material and dividing by 100. However, if this value is divided by the yield and then multiplied by 100, it would represent the percentage of the polymer relative to the solid phase.

**Table 1.** Chemical Composition and Higher Calorific Value (HCV) of Clone AF2 of *Populus euroamericana*, and Comparison with Other Materials.

| Composition                     | (1)             | (2)            | (3)             | (4)             | (5)             | (6)             | (7)             | (8)            |
|---------------------------------|-----------------|----------------|-----------------|-----------------|-----------------|-----------------|-----------------|----------------|
| $\alpha$ Cellulose (glucan) (%) | 40.3 $\pm$ 0.85 | 41.1 $\pm$ 2.1 | 38.9 $\pm$ 3.4  | 38.0 $\pm$ 2.4  | 44.0 $\pm$ 3.3  | 42.8 $\pm$ 2.0  | 33.8 $\pm$ 1.6  | 55.4 $\pm$ 2.6 |
| Klason Lignin (%)               | 25.1 $\pm$ 0.16 | 24.1 $\pm$ 1.8 | 19.8 $\pm$ 1.9  | 19.0 $\pm$ 2.5  | 27.8 $\pm$ 1.1  | 21.2 $\pm$ 0.9  | 19.9 $\pm$ 0.5  | 16 $\pm$ 0.3   |
| Xylan (%)                       | 19.3 $\pm$ 0.09 | 17.0 $\pm$ 0.5 | 19.9 $\pm$ 1.3  | 15.7 $\pm$ 0.1  | 15.7 $\pm$ 0.2  | 17.1 $\pm$ 0.3  | 23.9 $\pm$ 0.1  | 34.6 $\pm$ 0.4 |
| Araban (%)                      | 0               | -----          | 0.6 $\pm$ 0.3   | 1.5 $\pm$ 0.3   | 1.1 $\pm$ 0.1   | 0.7 $\pm$ 0.1   | 0.37 $\pm$ 0.2  | 5.6 $\pm$ 0.3  |
| Acetyl groups (%)               | 0.7 $\pm$ 0.02  | -----          | 4.4 $\pm$ 0.6   | 3.3 $\pm$ 0.5   | 4.4 $\pm$ 0.2   | 3.5 $\pm$ 0.1   | 4.32 $\pm$ 0.1  | -----          |
| HHV, KJUL/kg od.b.              | 19,982 $\pm$ 30 | -----          | 19,592 $\pm$ 28 | 18,981 $\pm$ 95 | 20,300 $\pm$ 53 | 19,326 $\pm$ 84 | 17,259 $\pm$ 25 | -----          |

Raw material percentages (100 kg dry matter); 1—Genus *Populus* (Poplar clone AF2). Present study; 2—Genus *Populus* [47]; 3—Tagasaste (*Chamaecytisus proliferus*) [49,50]; 4—Leucaena (*Leucaena diversifolia*) [51,52]; 5—Paulownia trihybrid (fortunei x tormentose x elongata) [53,54]; 6—*Eucalyptus globulus* [55,56]; 7—Sunflower stalks [52]; 8—Wheat straw [57].

**Table 2.** Normalized values of the process variables and composition of the solid fractions obtained in the two processes of cold alkaline extraction with and without ultrasound assistance of the *Populus x euroamericana* (Clone AF2). Additionally, the glucan, xylan, and lignin contents are expressed as percentages relative to the raw material.

| Variables |       |       | With Ultrasound |            |           |                   | Without Ultrasound |            |           |                   |
|-----------|-------|-------|-----------------|------------|-----------|-------------------|--------------------|------------|-----------|-------------------|
| $X_A$     | $X_t$ | $X_T$ | Yield (%)       | Glucan (%) | Xylan (%) | Klason Lignin (%) | Yield (%)          | Glucan (%) | Xylan (%) | Klason Lignin (%) |
| 0         | 0     | 0     | 68.8            | 86.4       | 40.4      | 67.0              | 73.2               | 89.8       | 45.4      | 88.5              |
| 0         | 0     | 0     | 68.8            | 86.4       | 40.4      | 67.0              | 73.2               | 89.8       | 45.4      | 88.5              |
| 1         | 1     | 1     | 63.3            | 80.4       | 45.0      | 58.4              | 68.5               | 93.2       | 56.8      | 80.1              |
| 1         | 1     | −1    | 67.9            | 84.3       | 43.5      | 62.4              | 77.8               | 95.7       | 49.3      | 83.4              |
| 1         | −1    | 1     | 69.0            | 84.8       | 49.5      | 73.9              | 73.3               | 96.5       | 54.7      | 97.5              |
| 1         | −1    | −1    | 75.0            | 95.8       | 50.2      | 67.4              | 80.8               | 98.2       | 47.4      | 90.6              |
| −1        | 1     | 1     | 64.7            | 96.2       | 47.2      | 51.5              | 69.3               | 98.1       | 43.3      | 71.6              |
| −1        | 1     | −1    | 70.9            | 96.2       | 51.6      | 66.7              | 77.6               | 98.2       | 51.3      | 90.9              |
| −1        | −1    | 1     | 69.5            | 85.7       | 49.9      | 69.2              | 71.6               | 89.8       | 53.0      | 89.5              |
| −1        | −1    | −1    | 74.6            | 87.6       | 55.7      | 77.7              | 78.5               | 92.1       | 60.2      | 98.9              |
| 1         | 0     | 0     | 67.3            | 91.0       | 44.4      | 60.9              | 72.7               | 98.7       | 47.4      | 79.7              |
| −1        | 0     | 0     | 69.4            | 95.6       | 50.3      | 61.3              | 73.1               | 97.4       | 47.6      | 79.6              |
| 0         | 1     | 0     | 66.5            | 81.7       | 39.2      | 68.7              | 73.7               | 88.1       | 46.4      | 93.3              |
| 0         | −1    | 0     | 71.0            | 84.6       | 44.2      | 74.4              | 75.4               | 85.1       | 52.0      | 98.1              |
| 0         | 0     | 1     | 68.6            | 82.1       | 40.9      | 68.4              | 71.1               | 86.3       | 49.5      | 90.6              |
| 0         | 0     | −1    | 73.5            | 84.1       | 42.6      | 72.9              | 78.7               | 87.8       | 50.1      | 96.0              |

$X_A$  alkali concentration,  $X_t$  time,  $X_T$  temperature.

The results were modeled using Equations (3)–(10) from Table 3, as described in Sections 2.2 and 2.3. By analyzing the residuals between the experimental (observed) values and those predicted by the polynomial multiple regression models, it was observed that the prediction errors were all less than 10% and, in some cases, even less than 5%. This percentage is understood as the percentage change within the range of each dependent variable, rather than as the percentage change in the maximum or minimum value. Therefore, the obtained values demonstrate the robustness of the models.

Also, the quadratic regression coefficients,  $R^2$ , all exceeded 0.95, which was considered acceptable given the simultaneous calculations involving several independent variables. The Snedecor's  $F$ -values significantly exceeded 5, which is the minimum value required to assume a good fit. All independent variables included in the models had individual Student's  $t$ -values greater than 2 or  $p$ -values less than 0.05, including their statistical significance at the 95% confidence level. For easier interpretation, the polynomial equations were employed to create the response surfaces in Figures 1 and 2 (refer to Section 2.3).

**Table 3.** Equations of the polynomial models for the dependent variables of the cold alkaline extraction (CAE) with and without ultrasound assistance of the *Populus x euroamericana* wood (Clone AF2).

| Equation with Ultrasounds  | Equation Number | Adjusted R <sup>2</sup> /Snedecor's F-Value |
|--|-----------------|---|
| YI = 68.5 − 0.67X <sub>A</sub> − 2.57X <sub>t</sub> − 2.66X <sub>T</sub> − 1.83X <sub>t</sub> <sup>2</sup> + 2.58X <sub>T</sub> <sup>2</sup>   | (3)             | 0.95/56                                     |
| GL = 87.0 − 2.50X <sub>A</sub> − 1.87X <sub>T</sub> + 5.98X <sub>A</sub> <sup>2</sup> − 4.03X <sub>T</sub> <sup>2</sup> − 4.39X <sub>A</sub> X <sub>t</sub> −<br>1.6X <sub>A</sub> X <sub>T</sub> + 1.19X <sub>t</sub> X <sub>T</sub>                      | (4)             | 0.98/59                                     |
| X = 40.2 − 2.28X <sub>A</sub> − 2.24X <sub>t</sub> − 1.12X <sub>T</sub> + 7.23X <sub>A</sub> <sup>2</sup> + 1.62X <sub>T</sub> <sup>2</sup> −<br>0.56X <sub>A</sub> X <sub>t</sub> + 1.37X <sub>A</sub> X <sub>T</sub> + 0.44X <sub>t</sub> X <sub>T</sub> | (5)             | 0.98/138                                    |
| KL = 66.6 − 5.96X <sub>t</sub> − 2.57X <sub>T</sub> − 5.33X <sub>A</sub> <sup>2</sup> + 4.58X <sub>T</sub> <sup>2</sup> + 1.04X <sub>A</sub> X <sub>t</sub> +<br>3.28X <sub>A</sub> X <sub>T</sub> − 2.34X <sub>t</sub> X <sub>T</sub>                     | (6)             | 0.98/114                                    |
| Equation without Ultrasounds   | Equation Number | Adjusted R <sup>2</sup> /Snedecor's F-Value |
| YI = 73.0 + 0.3 X <sub>A</sub> − 1.38 X <sub>t</sub> − 3.97X <sub>T</sub> + 1.68X <sub>T</sub> <sup>2</sup> − 0.57X <sub>A</sub> X <sub>t</sub> −<br>0.42X <sub>t</sub> X <sub>T</sub>   | (7)             | 0.98/202                                    |
| GL = 89.7 + 0.67X <sub>A</sub> + 1.16X <sub>t</sub> − 0.80X <sub>T</sub> + 8.37X <sub>A</sub> <sup>2</sup> − 2.86X <sub>T</sub> <sup>2</sup> −<br>2.53X <sub>A</sub> X <sub>t</sub>  | (8)             | 0.99/189                                    |
| X = 45.2 − 2.02X <sub>t</sub> + 2.39X <sub>A</sub> <sup>2</sup> + 4.39X <sub>T</sub> <sup>2</sup> + 2.84X <sub>A</sub> X <sub>t</sub> + 3.76X <sub>A</sub> X <sub>T</sub>  | (9)             | 0.99/211                                    |
| KL = 88.04 − 6.08X <sub>t</sub> − 3.05X <sub>T</sub> − 8.14X <sub>A</sub> <sup>2</sup> + 2.61X <sub>t</sub> <sup>2</sup> + 5.24X <sub>T</sub> <sup>2</sup> +<br>4.05X <sub>A</sub> X <sub>T</sub> − 2.75X <sub>t</sub> X <sub>T</sub>                      | (10)            | 0.99/251                                    |

Dependent variables: YI yield (%), GL glucan (%), X xylan (%), KL Klason lignin (%). Independent variables: X<sub>A</sub>: alkali concentration, X<sub>t</sub> and X<sub>T</sub>: treatment time and temperature. The differences between the experimental values and those estimated using the equations never exceeded 10% of the former.

The values predicted by the quadratic Equations (3)–(15) can be easily calculated using these equations and, as mentioned, replicate the experimental results with coefficients of variation below 10% of the range of variation of each dependent variable.

Before delving into the data in Tables 2 and 3, it is important to note that our initial hypothesis was confirmed (i.e., clone AF2 of *Populus x euramericana* proved a suitable raw material for the intended purpose). The CAE yields obtained in the absence of ultrasound were significantly higher than those obtained by Carvalho et al., 2016, and Fernández et al., 2020 [20,58] with eucalyptus (ranging 3.2% to 5.0%), but lower than those observed for grassy materials such as wheat (ranging from 25.5% 38.8%; [16,21]). A lower yield implies a higher extraction yield in the liquid phase. These results are consistent with our earlier discussion on the introduction that CAE efficiency depends on the specific raw material. For instance, eucalyptus wood, which is resistant to CAE fractionation [20], can be efficiently extracted at temperatures, such as those used by Alfaro et al., 2010, and Carvalho et al., 2016 [20,49], which reached temperatures of up to 175 °C, resulting in yields of 5.0% to 32.9%. This confirmation aligns with the proportions of different polymers extracted in our study.

Based on Equations (3) and (7) in Table 3, it is evident that temperature had the most significant impact on yield as an individual operational variable, both in the presence and absence of ultrasound. Figures 1A and 2A depict a similar response to the other two independent variables, although over considerably different ranges, ranging from 63.3% to 75.0% with sonication and from 68.5% to 80.8% without it. These findings underscore the pronounced influence of ultrasound on CAE yield. Indeed, experimental yields were notably lower with ultrasound, which was reflected in their mean values and the predictions made by the multiple regression models presented in Equations (3) and (7), particularly at the central points of the experimental design (68.5% with ultrasound and 73.0% without it). It is important to note that a lower yield was preferable as CAE efficiently removed structural components (cellulose, hemicellulose, and lignin) from the raw material. In fact, ultrasound-assisted CAE removed 25.0% to 36.7% of these initial structural components present in the material.

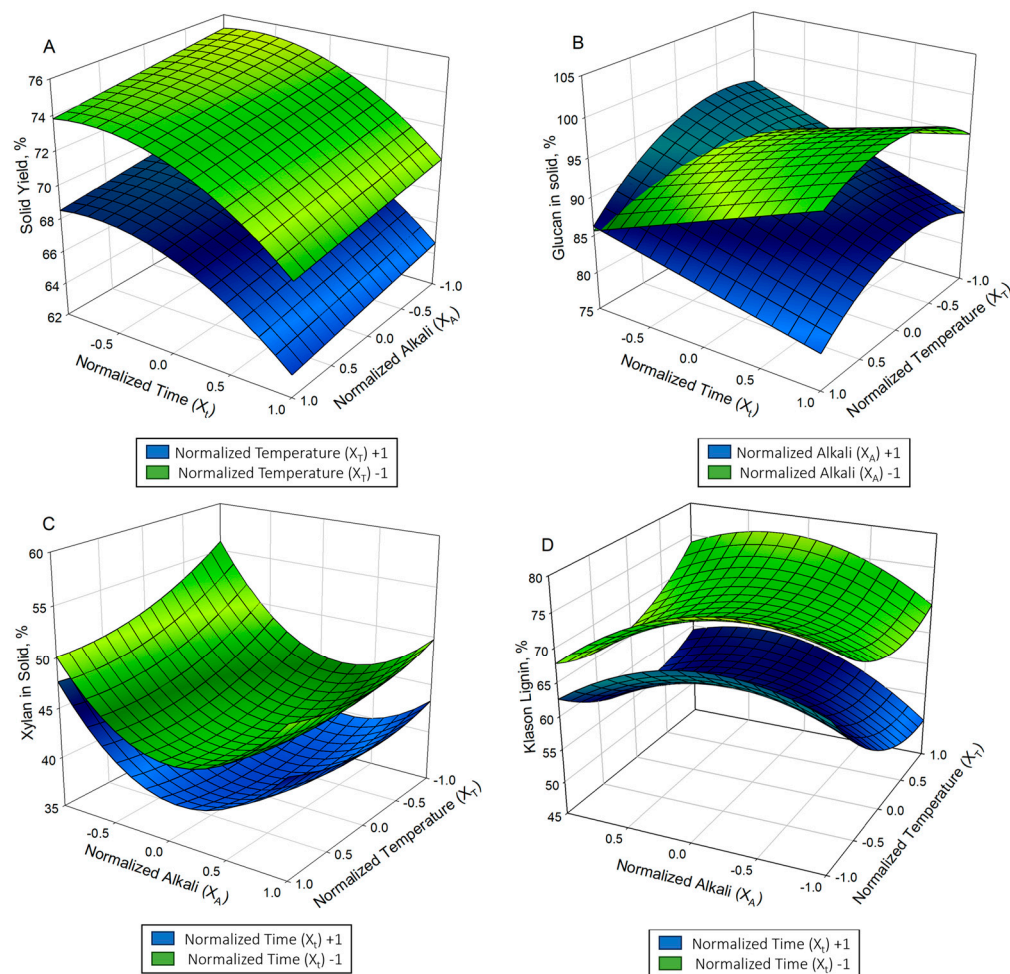


**Figure 1.** Surface responses for yield (A), as well as the glucan (B), xylan (C), and lignin contents (D) (percentage relative to the polymer content in raw material) in the solid residue obtained from the process of Cold Alkaline Extraction using ultrasound on the Poplar Wood (clone AF2).

As observed in the glucan surface responses shown in Figures 1 and 2, the glucan content of the CAE solid residue decreased with increasing alkali concentration, treatment time, and solid yield. However, according to Equations (4) and (8), the alkali concentration was the most influential variable on the glucan content. Furthermore, the difference between the predicted values for glucan content at the central point of the experimental design (87.0% with ultrasound and 89.7% without it) was much smaller than that of the corresponding mean yields. Therefore, the yield ranges, both with (81.7%–95.6%) and without ultrasound (85.1%–98.7%), were more similar. Therefore, as previously found by García et al., 2013, and Carvalho et al., 2016 [20,21], ultrasound had a notably selective effect on the hemicellulose and lignin fractions. This was particularly true for xylan, the primary component of the hemicellulose fraction, characterized by its low polymerization and non-crystallinity structure that makes it more susceptible to decomposition into monosaccharides. These findings support the initial hypothesis that ultrasound enhances hemicellulose extraction in the CAE liquor while preserving or even increasing the calorific potential of the solid residue.

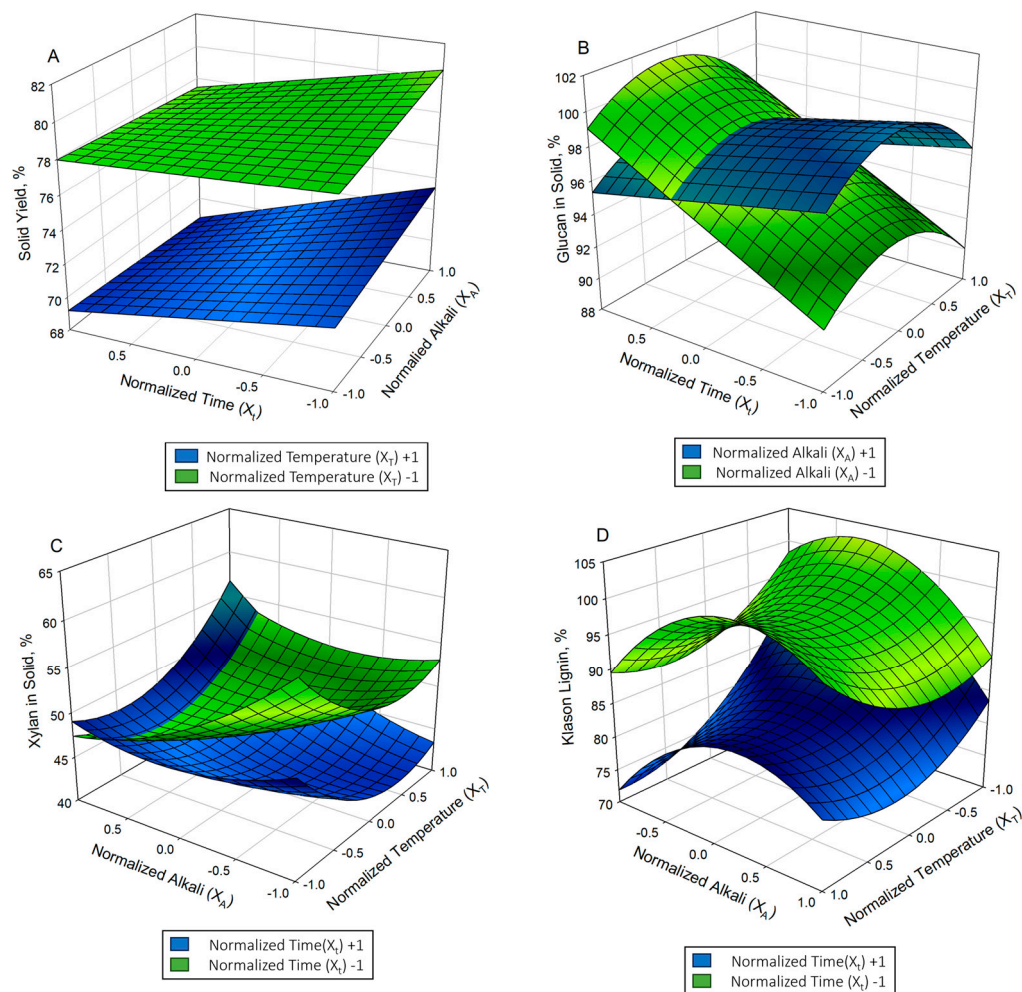


**Figure 2.** Surface responses for yield (A), as well as the glucan (B), xylan (C), and lignin contents (D) (percentage relative to the polymer content in raw material) in the solid residue obtained from the process of Cold Alkaline Extraction without ultrasound on the Poplar Wood (clone AF2).

In fact, when comparing the experimental ranges for hemicelluloses (xylan) extraction in the presence and absence of ultrasound (44.3%–60.8% vs. 39.8%–56.7%) with the predicted values at the central points based on Equations (5) and (9) (59.8% and 54.8%, respectively), it becomes evident that CAE had a much more selective effect on the hemicellulose fraction (xylan) than on the cellulose fraction (glucan). This difference was even more pronounced in the presence of ultrasound. This suggests that, notably, the CAE process exhibits a high selectivity for hemicelluloses while preserving the integrity of glucan. Alkaline treatments typically alter the structure of lignocellulosic materials by reducing the crystallinity and degree of polymerization of cellulose, thereby increasing the inner surface area, and facilitating release into the extraction medium [59].

Equations (6) and (10) do not provide a clear indication of the independent variable with the strongest influence on hemicellulose extraction into the CAE liquor. Figures 1C and 2C represent extreme values of treatment time, as it was clearly the independent variable that most strongly influenced CAE yield in a linear manner, without ultrasound. In the presence of ultrasound, the highest xylan contents of the solid residue (i.e., the lowest extraction of xylan into the CAE liquor) were achieved with extended treatment times, moderate alkali concentrations, and temperatures. The alkali concentration had little influence. Xylan extraction without ultrasound yielded similar results, although with lower hemicellulose extraction levels. These results were considerably higher than those reported by Carvalho et al., 2016 and Fernández et al., 2018 [20,60] for eucalyptus

(46%) but comparable to those of García et al., 2013, and Madejón et al., 2016 [16,21] for wheat straw.

In theory, preserving glucan integrity while maximizing hemicellulose extraction into the CAE liquor would be easiest by using a long treatment time, a medium temperature, and a medium-to-high alkali concentration. Below are described the results of the elemental analysis of the CAE solid residue in the presence of ultrasound to confirm the practicality of these operating conditions.

Obviously, preserving most of the glucan in the raw material in the CAE solid residue is of interest when considering the thermal stability of this component. In fact, the cellulose fraction has the highest energy content among the constituents of lignocellulosic biomass [60].

The amount of lignin remaining in the solid was also interest. Cold alkaline extraction partially delignifies the raw material, potentially facilitating subsequent delignification of the solid residue, making it useful for applications such as cellulose pulping, or increasing energy production through thermochemical treatment. Lignin acts as a seal protecting the lignocellulosic fraction, which needs to be broken down to fully exploit the raw material. Due to its abundance of benzene rings, lignin has the highest activation energy and thermal stability [61]. The use of ultrasound significantly facilitated its extraction. Delignification at the central point of the experimental design was estimated to be 33.4% in the presence of ultrasound and 12.0% in its absence (Table 3). Lignin was extracted by 22.3%–48.5% with ultrasound and 1.9%–28.4% without it (Table 2). However, lignin was consistently extracted to a lesser extent than hemicelluloses, indicating that CAE was less selective toward the lignin fraction. Therefore, longer treatment times at the upper end of the range (Equations (4) and (8)), along with medium temperatures (Figure 1D) and alkali concentrations (Figure 2D), may be suitable for effective delignification and hemicellulose extraction while preserving glucan integrity. Since lignin is the most structurally complex component and resistant to extraction from lignocellulosic materials, the treatment time will be especially influential on the efficiency of the chemical treatment and the cavitation effects of ultrasound, leading to cleavage of lignin–cellulose bonds [62].

In summary, these comparisons regarding the yield, glucan, hemicelluloses, and lignin content in the CAE processes with and without ultrasound assistance confirm the initial hypothesis and demonstrate a significant synergistic effect when ultrasound and CAE are applied simultaneously, enhancing both the selectivity and efficiency of hemicellulose extraction and the potential for increased energy yield from the post-treatment solid phase.

Another interesting point is the dependence of the elemental composition of the CAE solid residue on the operating conditions in the presence of ultrasound. This information can be useful for identifying the optimal operating conditions for extracting hemicelluloses from the target clone. The results are presented in Table 4, along with the lower heating value (LHV) (it is considered that the water vapor generated during combustion does not condense into liquid water, unlike in the case of higher heating value, where vapor condensation is taken into account) and moisture content. Table 5 displays the equations of the polynomial models derived from these results. Figure 3 illustrates the response surfaces for the contents in C, H, S and O, while Figure 4 shows the response surface for LHV.

**Table 4.** Values of the process variables and elemental composition (hydrogen, H; Sulphur, S; Carbon, C; and Oxygen, O) of the solid fractions obtained in the Cold alkaline extraction (CAE) with and without the use of ultrasound on *Populus x euroamericana* wood (Clone AF2).

| Normalized Values |       |       | Cold Alkaline Extraction (CAE) with Ultrasound |         |       |       |              |                                     |
|-------------------|-------|-------|--|---------|-------|-------|--------------|-------------------------------------|
| $X_A$             | $X_t$ | $X_T$ | H (%)  | S (%)   | C (%) | O (%) | Moisture (%) | LHV at Constant Volume (J/g o.d.b.) |
| 0                 | 0     | 0     | 6.105  | 0.00018 | 45.60 | 47.19 | 9.9          | 18,843                              |
| 1                 | 1     | 1     | 5.867  | 0.00000 | 41.01 | 52.03 | 8.2          | 19,233                              |
| 1                 | 1     | −1    | 5.872  | 0.00000 | 42.36 | 50.68 | 7.8          | 19,033                              |

Table 4. Cont.

| Normalized Values |       |       | Cold Alkaline Extraction (CAE) with Ultrasound |          |        |       |              |                                     |
|-------------------|-------|-------|--|----------|--------|-------|--------------|-------------------------------------|
| $X_A$             | $X_t$ | $X_T$ | H (%)  | S (%)    | C (%)  | O (%) | Moisture (%) | LHV at Constant Volume (J/g o.d.b.) |
| 1                 | −1    | 1     | 5.918  | 0.00024  | 44.70  | 48.23 | 10.0         | 18,115                              |
| 1                 | −1    | −1    | 5.922  | 0.00011  | 45.18  | 47.81 | 8.1          | 18,570                              |
| −1                | 1     | 1     | 5.841  | 0.00000  | 42.00  | 51.07 | 11.2         | 18,504                              |
| −1                | 1     | −1    | 5.858  | 0.00016  | 43.88  | 49.17 | 8.2          | 18,530                              |
| −1                | −1    | 1     | 5.861  | 0.00020  | 43.85  | 49.20 | 10.0         | 18,516                              |
| −1                | −1    | −1    | 5.908  | 0.00032  | 44.15  | 48.86 | 8.9          | 18,675                              |
| 1                 | 0     | 0     | 6.023  | 0.00014  | 44.00  | 49.01 | 11.2         | 18,965                              |
| −1                | 0     | 0     | 5.981  | 0.00030  | 44.25  | 48.71 | 8.8          | 18,872                              |
| 0                 | 1     | 0     | 5.972  | 0.00004  | 44.69  | 48.25 | 8.2          | 18,734                              |
| 0                 | −1    | 0     | 5.962  | 0.000140 | 45.547 | 47.4  | 8.1          | 18,477                              |
| 0                 | 0     | 1     | 5.870  | 0.000165 | 44.359 | 48.78 | 9.8          | 18,482                              |
| 0                 | 0     | −1    | 5.890  | 0.000205 | 45.076 | 47.78 | 9.7          | 18,686                              |

Table 5. Equations of the polynomial models for the dependent variables of the cold alkaline extraction (CAE) with ultrasound assistance of the clone AF2 of *Populus euroamericana*.

| Equation with Ultrasounds  | Equation Number | Adjusted $R^2$ /Snedecor's $F$ -Value |
|--|-----------------|---------------------------------------|
| $H = 6.100 + 0.015X_A - 0.016X_t - 0.093X_A^2 + 0.092X_t^2 - 0.220X_T^2$   | (11)            | 0.96/70                               |
| $S = 0.000180 - 0.000049X_A - 0.000086X_t - 0.000019X_T + 0.000036X_A^2 - 0.000089X_t^2 + 0.000050X_AX_T - 0.000023X_tX_T$ | (12)            | 0.95/40                               |
| $C = 45.62 - 1.02X_t - 0.470X_T - 1.514X_A^2 - 0.711X_T^2 - 0.549X_AX_t - 0.363X_tX_T$                                     | (13)            | 0.97/77                               |
| $O = 47.22 + 1.04X_t + 0.50X_T + 1.60X_A^2 + 0.81X_T^2 + 0.56X_AX_t$   | (14)            | 0.97/79                               |
| $LHV = 18,881 + 82X_A + 186X_t - 64X_T - 251X_T^2 + 217X_AX_t + 90X_tX_T$  | (15)            | 0.95/27                               |

Dependent variables: Hydrogen (%), Sulphur (%), Carbon (%), Oxygen (%), and LHV Low heating value. Independent variables:  $X_A$ : alkali concentration,  $X_t$  and  $X_T$ : treatment time and temperature of the cold alkaline extraction (CAE) with ultrasound of the target clone. The differences between the experimental values and those estimated using the equations never exceeded 10% of the former.

As shown in Figure 3A, the lowest hydrogen contents in the solid residues from ultrasound-assisted CAE were obtained at extreme temperatures and were scarcely dependent on the other independent variables. The sulfur content exhibited a similar behavior to the extraction yield and glucan content; thus, it decreased with increasing values of the three independent variables. In contrast, the carbon and oxygen contents increased with rising temperature, alkali concentration, and treatment time. This is consistent with the fact that the latter was a derivative quantity, and the former was the major element. The amount of carbon present in the CAE solid residue peaked at treatment times in the lower end of the range, where the temperature and alkali concentration had little influence, even though the highest carbon contents in the residue were obtained in the central ranges of the two variables. Since the carbon and hydrogen contents have contradictory effects on LHV, it is uncertain whether it is better to use treatment times in the lower or upper end of the range. Nevertheless, medium temperatures and alkali concentrations are the best choices to maximize LHV.

The H and C contents influence the calorific value of the material. LHV should increase with a decrease in H content and an increase in C content—although the former element is present in much smaller amounts than C. As demonstrated by Equation (11) in Table 5, the quadratic term of temperature had the most significant impact on the H content of the CAE solid residue obtained with ultrasound. Additionally, the lowest H contents were observed at low temperatures, regardless of the alkali concentration and treatment time employed. Nonetheless, the highest lower heating values, and consequently the greatest energy output, were achieved with longer treatment times, along with medium temperatures and alkali concentrations.

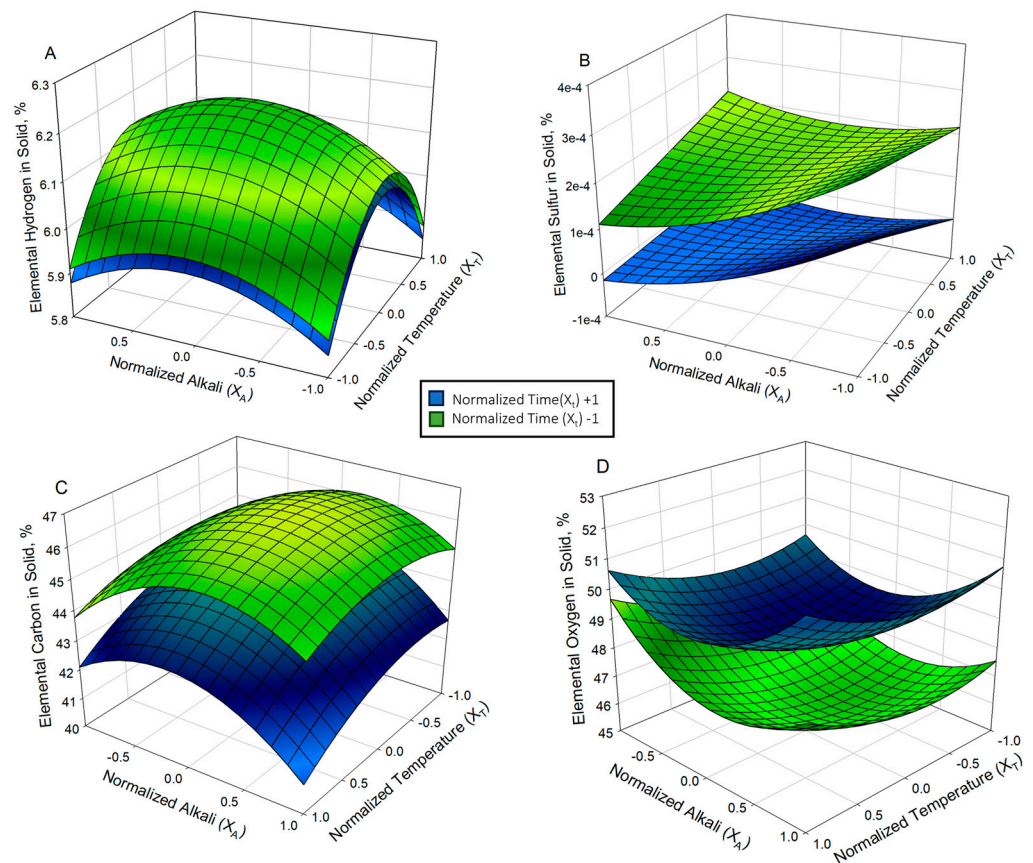


**Figure 3.** Response surfaces for elemental hydrogen (A), sulfur (B), carbon (C), and oxygen (D), all presented as percentages in the solid residue obtained from the Cold Alkaline Extraction process using ultrasound on the Popular Wood (clone AF2).

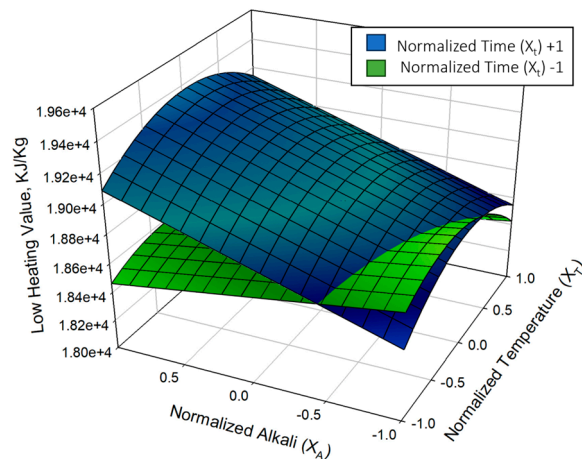


**Figure 4.** Response surface for lower heating values in the solid residue from the Cold Alkaline Extraction process using ultrasound on the Popular Wood (clone AF2).

Overall, utilizing extended durations, medium-to-high alkali concentrations, and moderate temperatures in conjunction with ultrasound yielded CAE solid residues with the highest glucan contents and lowest lignin contents. It also maximized hemicellulose extraction into the CAE liquor and the energy content (LHV) of the solid residue.

One other noteworthy point is the influence of ultrasound on LHV and the hemicellulose content of the CAE solid residue. As depicted in Figure 5, illustrating their variations at a constant treatment time (90 min, +1), it becomes evident that LHV was significantly

influenced by the presence of ultrasound. Therefore,  $LHV = 20,880 - 44.85 \times \text{hemicellulose content of solid}$  (Equation (16)) ( $R^2 = 0.79$ ). When ultrasound was employed, longer treatment times increased LHV and reduced the proportion of hemicelluloses in the CAE solid residue, subsequently increasing their concentration in the liquor. The effect was more pronounced at medium temperatures and, to a somewhat lesser extent, at medium alkali concentrations.

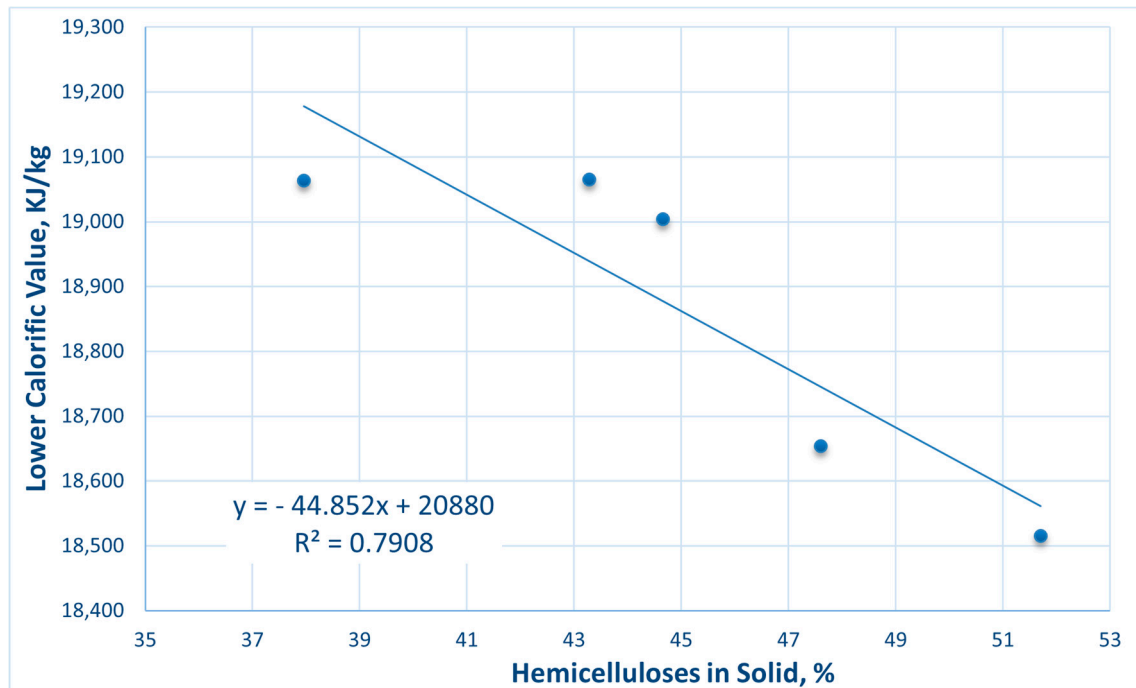


**Figure 5.** Predicted LHV (Equation (15)) against predicted xylan content (Equation (5)) of the solid residue obtained from the process of Cold Alkaline Extraction using ultrasound of the Poplar Wood (clone AF2) at a constant treatment time of 90 min (experimental point, normalized time value = +1).

#### 4. Conclusions

Clone AF2 of *Populus x euramericana* was found to have lignin and xylan contents slightly higher than those of *Eucalyptus globulus* and other species containing large amounts of biomass. Also, in common with other *Populus* species, the hemicellulose fraction of the clone contained no arabinan derivatives. However, its lower heating value (LHV) was considerably higher than that of *E. globulus* and other energy crops, and, unlike that of *Eucalyptus*, which was used as a reference here, it is suitable for the cold alkaline extraction (CAE) of hemicelluloses.

Using ultrasound increased the selectivity of CAE toward the hemicellulose and lignin fractions in the raw material. Thus, it increased hemicellulose extraction into the liquor while preserving or increasing the calorific value of the solid residue due to the cellulose fraction remaining in it.

The optimal conditions vary depending on the performance and property indices. However, overall, utilizing extended treatment times, medium-to-high alkali concentrations, and moderate temperatures with ultrasound-assisted CAE maximized the glucan content and minimized the lignin content of the resulting solid residue. It also maximized the extraction of hemicelluloses into the liquor and the energy content (LHV) of the solid residue.

**Author Contributions:** S.L.-C.: Conceptualization, Methodology, Investigation, Formal analysis, Data curation, Visualization, review. J.M.L.: Conceptualization, Methodology, Investigation, Formal analysis, Data curation, Visualization. J.C.G.: Conceptualization, Methodology, Funding acquisition, Supervision, Writing—review and editing. M.T.G.: Conceptualization, Methodology, Investigation, Formal analysis, Data curation, Visualization. F.L.: Conceptualization, Methodology, Data curation, Funding acquisition, Supervision, Writing—original draft, Project administration. All authors have read and agreed to the published version of the manuscript.

**Funding:** This work was funded by Spain’s Ministry of Science and Innovation, and also by the National Research Program Oriented to the Challenges of Society (Project PID2020-112875RB-C21, MCIN/AEI /10.13039/501100011033), also this publication is part of the PRE2021-097925 support (funded by MCIN/AEI/10.13039/501100011033 and by the FSE+), and the University of Huelva/CBUA.

**Data Availability Statement:** All data generated or analyzed during this work are included in this published article.

**Conflicts of Interest:** The authors declare that they have no competing interests.

## References

1. European Parliament. Directive (EU) 2018/2001 of the European Parliament and of the Council on the promotion of the use of energy from renewable sources. *Off. J. Eur. Union* **2018**, *2018*, 82–209.
2. REN21. *Renewables 2020 Global Status Report*; Renewable and Sustainable Energy Reviews; REN21 Secretariat: Paris, France, 2020; ISBN 978-3-948393-00-7. Available online: <https://www.ren21.net/gsr-2020/> (accessed on 11 December 2023).
3. Domínguez, E.; Nóvoa, T.; del Río, P.G.; Garrote, G.; Romani, A. Sequential two-stage autohydrolysis biorefinery for the production of bioethanol from fast-growing Paulownia biomass. *Energy Convers. Manag.* **2020**, *226*, 113517. [[CrossRef](#)]
4. Ginni, G.; Kavitha, S.; Kannah, Y.; Bhatia, S.K.; Kumar, A.; Rajkumar, M.; Kumar, G.; Pugazhendhi, A.; Chi, N.T.L. Valorization of agricultural residues: Different biorefinery routes. *J. Environ. Chem. Eng.* **2021**, *9*, 105435. [[CrossRef](#)]
5. World Energy Outlook 2017 [Internet]. OECD, 2017. Available online: [https://www.oecd-ilibrary.org/energy/world-energy-outlook-2017\\_weo-2017-en](https://www.oecd-ilibrary.org/energy/world-energy-outlook-2017_weo-2017-en) (accessed on 11 May 2021).
6. Seserman, D.-M.; Pohle, I.; Veste, M.; Freese, D. Simulating climate change impacts on hybrid-poplar and black locust short rotation coppices. *Forests* **2018**, *9*, 419. [[CrossRef](#)]
7. Montero, G.; Serrada, R. *La Situación de los Bosques y el Sector Forestal en España*; ISFE: Pontevedra, Spain, 2013.
8. del Mar Contreras, M.; Romero, I.; Moya, M.; Castro, E. Olive-derived biomass as a renewable source of value-added products. *Process Biochem.* **2020**, *97*, 43–56. [[CrossRef](#)]
9. Ning, P.; Yang, G.; Hu, L.; Sun, J.; Shi, L.; Zhou, Y.; Wang, Z.; Yang, J. Recent advances in the valorization of plant biomass. *Biotechnol. Biofuels* **2021**, *14*, 102. [[CrossRef](#)]
10. Cristóbal, J.; Matos, C.T.; Aurambout, J.P.; Manfredi, S.; Kavalov, B. Environmental sustainability assessment of bioeconomy value chains. *Biomass Bioenergy* **2016**, *89*, 159–171. [[CrossRef](#)]
11. Ruiz, H.A.; Conrad, M.; Sun, S.N.; Sanchez, A.; Rocha, G.J.M.; Romani, A.; Castro, E.; Torres, A.; Rodríguez-Jasso, R.M.; Andrade, L.P.; et al. Engineering aspects of hydrothermal pretreatment: From batch to continuous operation, scale-up and pilot reactor under biorefinery concept. *Bioresour. Technol.* **2020**, *299*, 122685. [[CrossRef](#)]
12. Sixto, H.; Cañellas, I.; van Arendonk, J.; Ciria, P.; Camps, F.; Sánchez, M.; Sánchez-González, M. Growth potential of different species and genotypes for biomass production in short rotation in Mediterranean environments. *For. Ecol. Manag.* **2015**, *354*, 291–299. [[CrossRef](#)]
13. FAO. *The Future of Food and Agriculture—Trends and Challenges*; FAO: Rome, Italy, 2017; ISBN 978-92-5-109551-5. Available online: <https://www.fao.org/3/i6583e/i6583e.pdf> (accessed on 11 December 2023).
14. Lauri, P.; Havlík, P.; Kindermann, G.; Forsell, N.; Böttcher, H.; Obersteiner, M. Woody biomass energy potential in 2050. *Energy Policy* **2014**, *66*, 19–31. [[CrossRef](#)]
15. Vangelova, E.; Pitman, R. Impacts of short rotation forestry on soil sustainability. Short rotation forestry: Review of growth and environmental impacts. *For. Res. Monogr.* **2011**, *2*, 37–77.
16. Madejón, P.; Alaejos, J.; García-Álbalá, J.; Fernández, M.; Madejón, E. Three-year study of fast-growing trees in degraded soils amended with composts: Effects on soil fertility and productivity. *J. Environ. Manag.* **2016**, *169*, 18–26. [[CrossRef](#)] [[PubMed](#)]
17. Madadi, M.; Song, G.; Karimi, K.; Zhu, D.; Elsayed, M.; Sun, F.; Abomohra, A. One-step lignocellulose fractionation using acid/pentanol pretreatment for enhanced fermentable sugar and reactive lignin production with efficient pentanol retrievability. *Bioresour. Technol.* **2022**, *359*, 127503. [[CrossRef](#)] [[PubMed](#)]
18. Penín, L.; Peleteiro, S.; Rivas, S.; Santos, V.; Parajó, J.C. Production of 5-hydroxymethylfurfural from pine wood via biorefinery technologies based on fractionation and reaction in ionic liquids. *Bioresources* **2019**, *14*, 4733–4747. [[CrossRef](#)]
19. Kim, J.S.; Lee, Y.Y.; Kim, T.H. A review on alkaline pretreatment technology for bioconversion of lignocellulosic biomass. *Bioresour. Technol.* **2016**, *199*, 42–48. [[CrossRef](#)]

20. de Carvalho, D.M.; Sevastyanova, O.; de Queiroz, J.H.; Colodette, J.L. Cold alkaline extraction as a pretreatment for bioethanol production from eucalyptus, sugarcane bagasse and sugarcane straw. *Energy Convers. Manag.* **2016**, *124*, 315–324. [CrossRef]
21. García, J.C.; Díaz, M.J.; Garcia, M.T.; Fera, M.J.; Gómez, D.M.; López, F. Search for optimum conditions of wheat straw hemicelluloses cold alkaline extraction process. *Biochem. Eng. J.* **2013**, *71*, 127–133. [CrossRef]
22. Hutterer, C.; Schild, G.; Potthast, A. A precise study on effects that trigger alkaline hemicellulose extraction efficiency. *Bioresour. Technol.* **2016**, *214*, 460–467. [CrossRef]
23. Park, Y.C.; Kim, J.S. Comparison of various alkaline pretreatment methods of lignocellulosic biomass. *Energy* **2012**, *47*, 31–35. [CrossRef]
24. Longue Júnior, D.; Colodette, J.L.; Gomes, V.J. Extraction of wood hemicelluloses through NaOH leaching | Remoção de hemiceluloses da madeira por tratamento de lixiviação alcalina com NaOH. *Cerne* **2010**, *16*, 423–429. [CrossRef]
25. Tiwari, B.K. Ultrasound: A clean, green extraction technology. *TrAC-Trends Anal. Chem.* **2015**, *71*, 100–109. [CrossRef]
26. Yuan, Z.; Long, J.; Wang, T.; Shu, R.; Zhang, Q.; Ma, L. Process intensification effect of ball milling on the hydrothermal pretreatment for corn straw enzymolysis. *Energy Convers. Manag.* **2015**, *101*, 481–488. [CrossRef]
27. Saikia, M.; Das, T.; Hower, J.C.; Silva, L.F.O.; Fan, X.; Saikia, B.K. Oxidative chemical beneficiation of low-quality coals under low-energy ultrasonic and microwave irradiation: An environmental-friendly approach. *J. Environ. Chem. Eng.* **2021**, *9*, 104830. [CrossRef]
28. Ashokkumar, M. The characterization of acoustic cavitation bubbles—An overview. *Ultrason. Sonochem.* **2011**, *18*, 864–872. [CrossRef] [PubMed]
29. García, A.; Alriols, M.G.; Llano-Ponte, R.; Labidi, J. Ultrasound-assisted fractionation of the lignocellulosic material. *Bioresour. Technol.* **2011**, *102*, 6326–6330. [CrossRef] [PubMed]
30. Raihan, A.; Ibrahim, S.; Muhtasim, D.A. Dynamic impacts of economic growth, energy use, tourism, and agricultural productivity on carbon dioxide emissions in Egypt. *World Dev. Sustain.* **2023**, *2*, 100059. [CrossRef]
31. Li, F.; Li, Y.; Novoselov, K.S.; Liang, F.; Meng, J.; Ho, S.-H.; Zhao, T.; Zhou, H.; Ahmad, A.; Zhu, Y.; et al. Bioresource Upgrade for Sustainable Energy, Environment, and Biomedicine. *Nano-Micro Lett.* **2023**, *15*, 35. [CrossRef]
32. Puişel, A.C.; Suditu, G.D.; Drăgoi, E.N.; Danu, M.; Ailiesei, G.-L.; Balan, C.D.; Chicet, D.-L.; Nechita, M.T. Optimization of Alkaline Extraction of Xylan-Based Hemicelluloses from Wheat Straws: Effects of Microwave, Ultrasound, and Freeze–Thaw Cycles. *Polymers* **2023**, *15*, 1038. [CrossRef]
33. Gufe, C.; Thantsha, M.S.; Malgas, S. Recovery of xylan from *Acacia mearnsii* using ultrasound-assisted alkaline extraction. *Biofuels Bioprod. Biorefining* **2023**, *17*, 976–987. [CrossRef]
34. Tareen, A.K.; Punsuvon, V.; Parakulsuksatid, P. Conversion of steam exploded hydrolyzate of oil palm trunk to furfural by using sulfuric acid, solid acid, and base catalysts in one pot. *Energy Sources Part A Recovery Util. Environ. Eff.* **2020**, 1–12. [CrossRef]
35. Gil, M.V.; Jablonka, K.M.; García, S.; Pevida, C.; Smit, B. Biomass to energy: A machine learning model for optimum gasification pathways. *Digit. Discov.* **2023**, *2*. [CrossRef]
36. Tofani, G.; Cornet, I.; Tavernier, S. Multiple linear regression to predict the brightness of waste fibres mixtures before bleaching. *Chem. Pap.* **2022**, *76*, 4351–4365. [CrossRef]
37. TAPPI T264 cm-07; Preparation of Wood for Chemical Analysis. TAPPI Press: Atlanta, GA, USA, 2007.
38. TAPPI 211 om-02; Ash in Wood, Pulp, Paper and Paperboard: Combustion at 525 °C. TAPPI Press: Atlanta, GA, USA, 2002.
39. TAPPI T204 cm-07; Solvent Extractives of Wood and Pulp. TAPPI Press: Atlanta, GA, USA, 2007.
40. TAPPI T249 cm-09; Carbohydrate Composition of Extractive-Free Wood and Wood Pulp by Gas-Liquid Chromatography. TAPPI Press: Atlanta, GA, USA, 2009.
41. Romani, A.; Garrote, G.; Ballesteros, I.; Ballesteros, M. Second generation bioethanol from steam exploded *Eucalyptus globulus* wood. *Fuel* **2013**, *111*, 66–74. [CrossRef]
42. TAPPI T222 om-11; Acid-Insoluble Lignin in Wood and Pulp. TAPPI Press: Atlanta, GA, USA, 2011.
43. CEN/TS Solid Biofuels-Method for the Determination of Calorific Value CEN/TS 14918:2005. 2005. Available online: <https://standards.iteh.ai/catalog/standards/cen/21f53010-bfdf-41aa-8f73-3ad9e2ab444f/cen-ts-14918-2005> (accessed on 11 December 2023).
44. UNE 16001 EX; Solid Biofuels, Method for the Determination of Calorific Value. Spanish Association for Standardization: Madrid, Spain, 2005. Available online: <https://infostore.saiglobal.com/preview/is/en/2005/i.s.cents14918-2005.pdf?sku=675235> (accessed on 11 December 2023).
45. Civitarese, V.; Faugno, S.; Picchio, R.; Assirelli, A.; Sperandio, G.; Saulino, L.; Crimaldi, M.; Sannino, M. Production of selected short-rotation wood crop species and quality of obtained biomass. *Eur. J. For. Res.* **2018**, *137*, 541–552. [CrossRef]
46. Magagnotti, N.; Spinelli, R.; Kärhä, K.; Mederski, P.S. Multi-tree cut-to-length harvesting of short-rotation poplar plantations. *Eur. J. For. Res.* **2020**, *140*, 345–354. [CrossRef]
47. Constantí, M.; Reguant, C.; Poblet, M.; Zamora, F.; Mas, A.; Guillamón, J.M. Molecular analysis of yeast population dynamics: Effect of sulphur dioxide and inoculum on must fermentation. *Int. J. Food Microbiol.* **1998**, *41*, 169–175. [CrossRef] [PubMed]
48. Ebringerová, A.; Hromádková, Z. An overview on the application of ultrasound in extraction, separation and purification of plant polysaccharides. *Cent. Eur. J. Chem.* **2010**, *8*, 243–257. [CrossRef]
49. Alfaro, A.; López, F.; Pérez, A.; García, J.C.; Rodríguez, A. Integral valorization of tagasaste (*Chamaecytisus proliferus*) under hydrothermal and pulp processing. *Bioresour. Technol.* **2010**, *101*, 7635–7640. [CrossRef]

50. López, F.; Alfaro, A.; García, M.; Díaz, M.J.; Calero, A.M.; Ariza, J. Pulp and paper from tagasaste (*Chamaecytisus proliferus* L.F. ssp. *palmensis*). *Chem. Eng. Res. Des.* **2004**, *82*, 1029–1036. [[CrossRef](#)]
51. Fera, M.J.; García, J.C.; Pérez, A.; Gomide, J.L.; Colodette, J.L.; López, F. Process optimization in kraft pulping, bleaching, and beating of *Leucaena diversifolia*. *Bioresources* **2012**, *7*, 283–297. [[CrossRef](#)]
52. Caparrós, S.; Ariza, J.; López, F.; Nacimiento, J.A.; Garrote, G.; Jiménez, L. Hydrothermal treatment and ethanol pulping of sunflower stalks. *Bioresour. Technol.* **2008**, *99*, 1368–1372. [[CrossRef](#)] [[PubMed](#)]
53. García, J.C.; Zamudio, M.A.M.; Pérez, A.; De Alva, H.E.; López, F. Paulownia as a raw material for the production of pulp by soda-anthraquinone cooking with or without previous autohydrolysis. *J. Chem. Technol. Biotechnol.* **2011**, *86*, 608–615. [[CrossRef](#)]
54. López, F.; Pérez, A.; Zamudio, M.A.M.; De Alva, H.E.; García, J.C. Paulownia as raw material for solid biofuel and cellulose pulp. *Biomass Bioenergy* **2012**, *45*, 77–86. [[CrossRef](#)]
55. Loaiza, J.M.; López, F.; García, M.T.; Fernández, O.; Díaz, M.J.; García, J.C. Selecting the pre-hydrolysis conditions for eucalyptus wood in a fractional exploitation biorefining scheme. *J. Wood Chem. Technol.* **2016**, *36*, 211–223. [[CrossRef](#)]
56. López, F.; García, M.; Fera, M.; García, J.; de Diego, C.; Zamudio, M.; Díaz, M. Optimization of furfural production by acid hydrolysis of eucalyptus globulus in two stages. *Chem. Eng. J.* **2014**, *240*, 195–201. [[CrossRef](#)]
57. Pan, X.; Sano, Y. Fractionation of wheat straw by atmospheric acetic acid process. *Bioresour. Technol.* **2005**, *96*, 1256–1263. [[CrossRef](#)]
58. Fernández, M.; Alaejos, J.; Andivia, E.; Madejón, P.; Díaz, M.J.; Tapias, R. Short rotation coppice of leguminous tree *Leucaena* spp. improves soil fertility while producing high biomass yields in Mediterranean environment. *Ind. Crops Prod.* **2020**, *157*, 112911. [[CrossRef](#)]
59. Hu, M.; Chen, Z.; Wang, S.; Guo, D.; Ma, C.; Zhou, Y.; Chen, J.; Laghari, M.; Fazal, S.; Xiao, B.; et al. Thermogravimetric kinetics of lignocellulosic biomass slow pyrolysis using distributed activation energy model, Fraser-Suzuki deconvolution, and iso-conversional method. *Energy Convers. Manag.* **2016**, *118*, 1–11. [[CrossRef](#)]
60. Fernández, M.; Alaejos, J.; Andivia, E.; Vázquez-Piqué, J.; Ruiz, F.; López, F.; Tapias, R. Eucalyptus x urograndis biomass production for energy purposes exposed to a Mediterranean climate under different irrigation and fertilisation regimes. *Biomass Bioenergy* **2018**, *111*, 22–30. [[CrossRef](#)]
61. Chen, Z.; Zhu, Q.; Wang, X.; Xiao, B.; Liu, S. Pyrolysis behaviors and kinetic studies on Eucalyptus residues using thermogravimetric analysis. *Energy Convers. Manag.* **2015**, *105*, 251–259. [[CrossRef](#)]
62. Methrath Liyakathali, N.A.; Muley, P.D.; Aita, G.; Boldor, D. Effect of frequency and reaction time in focused ultrasonic pretreatment of energy cane bagasse for bioethanol production. *Bioresour. Technol.* **2016**, *200*, 262–271. [[CrossRef](#)] [[PubMed](#)]

**Disclaimer/Publisher’s Note:** The statements, opinions and data contained in all publications are solely those of the individual author(s) and contributor(s) and not of MDPI and/or the editor(s). MDPI and/or the editor(s) disclaim responsibility for any injury to people or property resulting from any ideas, methods, instructions or products referred to in the content.